RevMexAA (Serie de Conferencias), **32**, 69–73 (2008)

THE BROAD LINE REGION OF QUASARS

Paola Marziani,[1] Jack W. Sulentic,[2] and Deborah Dultzin[3]

RESUMEN

A lo largo de la década pasada se avanzó mucho en nuestra comprensión sobre las propiedades espectroscópicas de los AGN (Núcleos Activos de Galaxias). Esta contribución revisa algunos resultados observacionales importantes obtenidos tanto en el óptico como en el UV, así como las restricciones impuestas sobre los parámetros físicos que controlan la estructura y la dinámica de la región que emite las líneas anchas.

ABSTRACT

The last decade saw long-awaited improvements in our understanding of active galactic nuclei (AGN) spectral properties. This contribution reviews some important observational results obtained from optical and UV data, as well as constraints on physical parameters that control the structure and dynamics of the Broad Line Region.

Key Words: black hole physics — galaxies: active — quasars: emission lines — quasars: general

1. INTRODUCTION

"A thousand spectra are worth more than one average spectrum" is perhaps an appropriate modern extension of the aphorism "a spectrum is worth a thousand pictures" – at least for active galactic nuclei (Cox 2000; Dultzin-Hacyan et al. 2000). The "one thousand" spectra of a source are needed to obtain an estimate of the spatial extent of the broad line emitting region (BLR). The time delay between line and continuum flux variations (i.e. reverberation) is $\lesssim$ 1 month, implying an angular size of just 0.1 marcsec at $z \approx 0.010$. Three orders of magnitude improvement in resolution is still needed to obtain a fuzzy view of the BLR with direct, space-borne optical imaging.

Monitoring several lines emitted by ionic species of widely different ionization levels would advance another, yet small step toward structure resolution. It is useful to separate lines into high ionization (HILs: $\gtrsim$ 40–50 eV): C IVλ1549, O IV]+Si IV λ1400, He IIλ1640, He IIλ4686 and low ionization (LILs: $\lesssim$ 20 eV): Balmer lines, Fe II, C II, Mg IIλ2800. A major effort in the 1990s established that HILs usually respond with shorter time-scales than LILs (see e.g., Korista et al. 1995, for NGC 5548). Unfortunately, studies of response in narrow radial velocity intervals across line profiles (i.e. 2D reverberation mapping) have slowed since then (but see Kollatschny 2003), not least because of technical difficulties demanding dedicated instrumentation (Horne et al. 2004).

Emission line properties of quasars do not scatter randomly with reasonable dispersion around an average, so that "one thousand" spectra are also needed to exploit spectral diversity as well as spectral variability. The range of observed H$\beta_{\rm BC}$ (where BC stands for Broad Component) FWHM spans more than one order of magnitude, from $\approx$ 800 km s^{-1}, to $\approx$ 20000 km s^{-1} in some extreme sources. The Fe II prominence parameter $R_{\rm FeII}$ (defined as the intensity of the Fe II blend centered at 4570 Å normalized by the intensity of H$\beta_{\rm BC}$) varies from almost 0 to $\approx$1.5–2.0 in large quasar samples (Sulentic, Marziani & Dultzin-Hacyan 2000).

2. DIFFERENCES IN BLR STRUCTURE AND KINEMATICS

Considering the diversity of quasar properties, it seems meaningful to average spectra in bins defined within the so-called "Eigenvector 1 optical plane" of the 4D Eigenvector 1 parameter space (4DE1, see Sulentic et al. 2008) or to separate at least narrower [FWHM(H$\beta_{\rm BC}$) $\leq$ 4000 km s^{-1}, Population A] and broader sources [Population B]. There is evidence in favor of two different BLR populations and of a meaningful limit at FWHM(H$\beta_{\rm BC}$) $\approx$ 4000 km s^{-1} (see Sulentic et al. 2007). The distinction between Population A and B may be more fundamental than either the radio quiet (RQ)-radio loud (RL) or the Narrow Line Seyfert 1 (NLSy1) vs. rest of quasars dichotomies. Several tests find no significant distributional difference between NLSy1s and sources

[1]INAF, Osservatorio Astronomico di Padova, Vicolo dell'Osservatorio 5, I-35122 Padova, Italy (paola.marziani @oapd.inaf.it).
[2]Department of Physics and Astronomy, University of Alabama, Tuscaloosa, AL 35487, USA (giacomo@merlot. astr.ua.edu).
[3]Instituto de Astronomía, Universidad Nacional Autónoma de México, Apdo. Postal 70-264, México, D. F. 04510, México (deborah@astroscu.unam.mx).

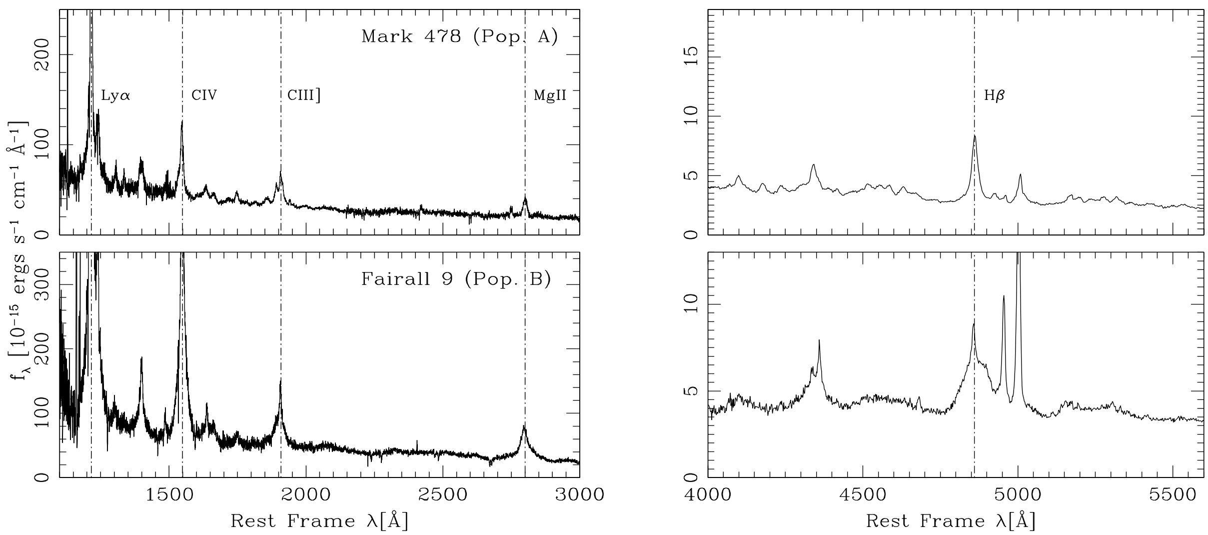

Fig. 1. HST/FOS (left panels) and optical, ground based spectra (right panels) of two representative sources: Mark 478 (Population A, top), and Fairall 9 (Population B, bottom). The strongest lines whose profiles are shown in the next figures are identified.

with FWHM(H$\beta_{\rm BC}$) in the range 2000–4000 km s^{-1}, suggesting that the 2000 km s^{-1} cutoff is artificial. Intriguing differences emerge if the Population A/B distinction is applied.

- Population A sources show Lorentzian H$\beta_{\rm BC}$ profiles, most often symmetric or with slight blueward asymmetry, while Population B sources show double Gaussian H$\beta_{\rm BC}$ profiles, often redward asymmetric (Sulentic et al. 2002, see also Figure 1).
- The C IVλ1549 profile is most often blueward asymmetric and blueshifted in Population A, and it becomes a double Gaussian, redward asymmetric or symmetric in Population B. The C IVλ1549 and H$\beta_{\rm BC}$ profiles appear to be more similar in Population B. (Sulentic et al. 2007, and references therein).

Figure 1 shows optical and UV spectra for typical Population A and B sources. A visual impression is that the ionization degree is higher for Population B (Marziani et al. 2001), with lower $R_{\rm FeII}$ and more prominent HILs. Kinematics and physical conditions may not be fully unrelated, for example if both Population A and B sources share a low-ionization region responsible for most or all of the Fe II emission, while a high-ionization, broader component is dominant in Population B only.

3. UV/OPTICAL SPECTROPHOTOMETRIC COMPARISON OF 2 PROTOTYPICAL SOURCES

Here, we consider two sources in detail, Mark 478 and Fairall 9, which are representative of Population A and Population B respectively (Figure 1). HST/optical data allow us to analyze all the strongest emission lines from Lyα to Hβ.

Mark 478 (Figure 2) – The H$\beta_{\rm BC}$ profile is well fit by a Lorentzian function. If we assume that emission with the same profile is also present in C IVλ1549 then C IVλ1549 can be decomposed into this component and a rather strong, blueshifted component. A similar deconvolution very successfully reproduces the Lyα profile. No blueshifted component is detected in Hβ. Mg IIλ2800 is fit by a double Lorentzian.

Fairall 9 (Figure 3) – H$\beta_{\rm BC}$ and MgIIλ2800 are well fit with two Gaussian components, one narrower/unshifted and the other one much broader and shifted to the red ("very broad component", VBC). Lyα and C IVλ1549 may be equally well-fit by two components. However, the VBC FWHM would be larger and the shift lower than in the case of Hβ and MgIIλ2800, suggesting the presence of a third component. We prefer to fit Lyα and C IVλ1549 as shown in Figure 3: a redshifted component analogous to the one identified in Hβ, and an additional blueshifted component.

A tentative nebular analysis can be carried out for the main components identified in the profile decomposition using `CLOUDY` photoionization computations (Ferland et al. 1998). `CLOUDY 7.0` incorporates a 287-level model of the Fe II ion following Verner et al. (1999). This is especially useful since we are

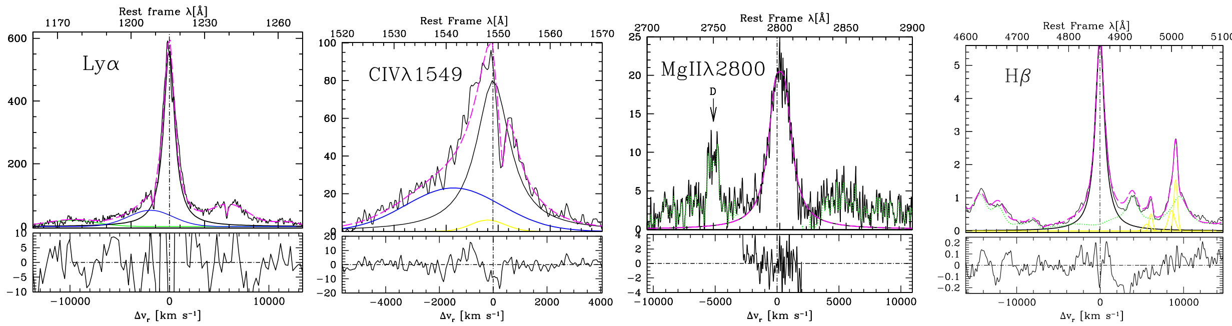

Fig. 2. Profile analysis results for Mark 478, the prototypical Population A source considered in this study. Ordinate is rest-frame specific flux in units of 10^{-15} ergs s^{-1} cm^{-2} Å^{-1}, corrected because of Galactic extinction. Dashed lines indicate sum of line model emission, dotted lines indicate Fe II emission. Due to the heavy Fe II contamination we only fit the doublet core of MgII. See text for further details.

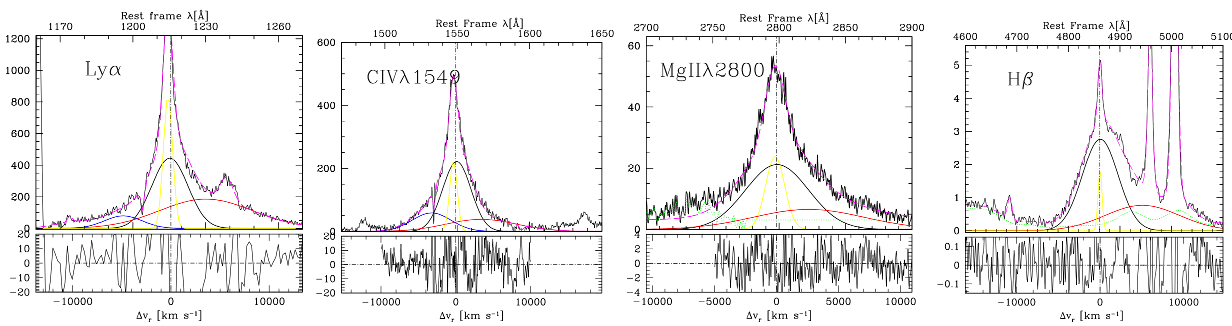

Fig. 3. Profile analysis results of Fairall 9 (Population B prototype). Units and meaning of symbols are the same of the previous Figure. Due to the non-simultaneity of the observations, and to the rather variable behavior of F 9 at the time the HST spectra were collected, it is not advisable to compare fluxes in the optical (Hβ) and UV lines.

able to measure the Fe II emission for the 2000–3000 Å range (Fe$_{\rm UV}$), at least normalized to Lyα. We attempt to reproduce the observed line ratios for the main components identified in the two sources always assuming $N_{\rm H} = 10^{23}$ cm^{-2}, standard AGN continuum, and solar abundances.

Mark 478: low ionization Lorentzian BC – A very low ionization component accounts for most emission in the Hβ spectral region. Emission line ratios are best fit if ionization parameter is $\log\Gamma \lesssim -2$ and electron density $\log n_{\rm e} \gtrsim 12$, where $n_{\rm e}$ is expressed in cm^{-3}. High density and low ionization are especially needed to account for $R_{\rm FeII} \approx 1$ and Fe II$_{\rm UV}$/Ly$\alpha \approx 1$. The very high $n_{\rm e}$ is supported by the ratio C IIIλ1176/Ly$\alpha \sim 0.1$.

Mark 478: blueshifted component – The blueshifted component in Mark 478 appears to be less well constrained, partly because it is very weak in the Hβ range and strong in the UV lines. Ionization is presumably high for the gas emitting this component ($\log\Gamma \sim -0.5 to - 1.0$) and density may be $\log n_{\rm e} \gtrsim 10-11$ although $N_{\rm H}$ may be substantially lower than assumed in our explorative calculations.

F 9: low ionization Gaussian BC – The lower ionization component, with narrower profile, is responsible for *all* of the Fe II emission, which is not negligible in F 9: Fe$_{\rm UV}$/Ly$\alpha \approx 0.4$, $R_{\rm FeII} \approx 0.7$ for this component only (the 4DE1 $R_{\rm FeII}$ includes all Hβ flux [minus the narrow component] and is ≈ 0.4). The observed ratios are best explained if $\log\Gamma \sim -2$, and $\log n_{\rm e} \sim 11-12$. These physical conditions are not much dissimilar from the ones deduced for the Lorentzian component of Mark 478 and, as expected, the C IIIλ1176 line is detected.

F 9: high ionization, redshifted very broad Gaussian component (VBC) – The absence of "very broad" Fe II emission, and the rather prominent "very broad" He IIλ 1640 suggest high ionization. This broader component can be accounted for by gas with ionization parameter $\log\Gamma \sim -0.5 to -$

1.0, and moderate electron density $\log n_{\rm e} \sim 9.5-10$. These parameters have been considered for a long time the canonical ones for the BLR.

F 9: blueshifted component – The high-ionization blueshifted component used to fit the Lyα and C IVλ1549 profiles (Figure 3) is interpreted as analogous to the one observed in Mark 478.

Optical Fe II emission is self-similar in almost all sources within common S/N ($\sim$ 100) and $\lambda/\Delta\lambda$ ($\sim 10^3$) limits (Marziani et al. 2003a). The results obtained so far suggest that the similarity of the optical Fe II spectrum across Population A and B is due to emission through photoionization of a very dense medium. The connection between kinematics and ionization degree seems to be related to the relative prominence of the high and low ionization components in the HILs and LILs, since it is the low ionization component that produces all Fe II emission. How can we tentatively account for the different line profiles and different average ionization conditions in Population A and B sources?

4. PHYSICAL PARAMETERS BEHIND THE OBSERVED BROAD LINE DIVERSITY

4.1. *Radio Loudness*

First, we consider whether a powerful, radio jet somehow affects the observational properties of the BLR. To this aim, we compared median H$\beta_{\rm BC}$ profiles of 56 RQ and 36 RL sources in the black hole mass ($M_{\rm BH}$) interval $8.5 < \log M_{\rm BH} < 9.5$ and unrestricted bolometric luminosity-to-mass $L/M_{\rm BH}$ ratio (Marziani et al. 2003b). Most of these will be Population B sources. The H$\beta_{\rm BC}$ profiles (after Fe II and narrow line subtraction) of RQ and RL sources are almost identical. The BLR (but not the Narrow Line Region!) does not seem to see whether a source is radio-loud or radio-quiet.

4.2. *Luminosity*

VLT/ISAAC data provide IR spectra with resolution and S/N similar to optical data. We observed 50 sources to cover redshifted Hβ (Sulentic et al. 2004, 2006). Luminous quasars in the range $1.0 \lesssim z \lesssim 2.5$ still show Population A and Population B characteristics. LIL equivalent widths and $R_{\rm FeII}$ do not appear to depend significantly on L, even on a $\Delta m \sim 10$ range. FWHM(H$\beta_{\rm BC}$) is expected to increase $\propto 10^{-0.08 M_{\rm B}}$ if broadening of H$\beta_{\rm BC}$ is due to virialized gas motions with $r_{\rm BLR} \propto L^{0.7}$ (see Sulentic et al. 2004, for details).

4.3. *Gravitational Redshift*

The centroid at 0 intensity $c(0/4)$ of H$\beta_{\rm BC}$ loosely correlates with $M_{\rm BH}$; the correlation is significant ($P \sim 10^{-3}$) because a very large sample of $\sim$ 300 sources has been considered. If gas motion remains virial down to the inner edge of the BLR there will be a simple relationship between the $c(0/4)$ and FWZI. The amplitude of redward asymmetry depends on $M_{\rm BH}$ but gravitational redshift seems to be statistically inadequate to produce the $c(0/4)$ redshifts. The difficulty is even more serious if the high-ionization VBC is considered alone.

4.4. *Aspect Angle*

The angle θ between the line of sight and the radio jet axis can be estimated equalling the observed X-ray flux at 1 KeV to the flux expected from the synchrotron self-Compton process acting on radio photons to obtain the Doppler factor. The Lorentz factor can be then retrieved from the apparent velocity if the source is superluminal (following Sulentic et al. 2003, and references therein). Orientation matters, affecting the FWHM(H$\beta_{\rm BC}$) by a factor $\approx$ 2. This technique can be applied only to quasars with detected superluminal motion. There is yet no known way to retrieve individual θs for the rest of AGN (Collin et al. 2006).

4.5. *Eddington Ratio and Black Hole Mass*

The H$\beta_{\rm BC}$ profiles change strongly as a function of Eddington ratio with profiles being generally Lorentzian if $\log L/M_{\rm BH} \gtrsim 3.9$ in solar units (Marziani et al. 2003b) and Gaussian or double-Gaussian below this limit. The mass $M_{\rm BH}$, estimated according to the virial assumption, yields second order effects, mainly in the line wings. The Eddington ratio also strongly affects high ionization lines like C IVλ1549: significant and large blueshifts ($\Delta v_{\rm r} \lesssim -500$ km s^{-1}) are confined to Population A sources only (Sulentic et al. 2007). These results suggest that the Population A/B separation is physically motivated and driven by Eddington ratio.

4.6. *Where is the Accretion Disk?*

Few ($\approx$ 2% in the SDSS), very broad sources, with FWHM $\sim$ 6 times the average FWHM of Balmer lines (Strateva et al. 2003), show double-peaked profiles that suggest accretion disk emission. To adjust the theoretical to the observed profiles, non-axisymmetric or warped disks are most often required. A two component models for the LILs, a disk (corresponding to the high ionization component described in this paper) plus a spherical one has been successful for 12 AGN, Population A and Population B. (Popović et al. 2004), but it is as yet unclear whether those results can be of general validity. Eddington ratios of double-peaked sources are much lower than those of typical type-1 AGN: $\lesssim 0.02$ in 90% (Wu & Liu 2004). Old criticism based on line profile shape for the wide majority of AGN is still standing (Sulentic et al. 1990): if only the accretion disk is emitting H$\beta_{\rm BC}$, we expect that at the line base the centroid shift is due to gravitational and transverse redshift, but this is not always the case, not even in Population B sources.

5. CONCLUDING REMARKS

Several BLR physical and kinematical properties seem to be governed primarily by the Eddington ratio. It was not so clear ten years ago. LILs properties are remarkably similar over a very wide range of luminosity, even at very high z, and broad line profile shapes (both LILs and HILs) show only second-order effects that can be directly ascribed to $M_{\rm BH}$. We have also learned with more assurance that the BLR appears to be transparent to radio loudness. This does not mean that RL and RQ samples show similar spectra: *only* Population B RQ quasars and lobe dominated RL quasar show very similar spectra, with low Fe II emission and broad H$\beta_{\rm BC}$ (Marziani et al. 1996; Dultzin-Hacyan et al. 2000). This may point toward a parallel evolution for RL and part of the RQ quasars: what makes them radio-different is an as yet unknown parameter that has little, if any, effect on their BLR.

We are still left with many conundrums concerning the actual origin of the BLR gas, its dynamics and spatial disposition. High-ionization gas (an accretion disk wind?), showing non-virial, outward motion and producing the blueshifted component observed in Mark 478 and, to a lesser extent, in F 9, may decrease in importance crossing the boundary from Population A, where it is strong in the HILs, to Population B where it may become almost hidden by the redshifted, very broad component. The central engine may sustain a most prominent outflow only if the Eddington ratio is relatively high, as in the case of Population A sources.

Placing these considerations on a firmer observational basis requires renewed efforts involving nebular diagnostics and line profile analysis, as well as the ability to understand how the viewing angle affects observed BLR parameters on a source-by-source basis, if we cannot count on 2D reverberation mapping. 4DE1 offers promise for decoupling source orientation from physics.

PM wishes to thank the SOC for inviting her to speak in Huatulco. It was a valuable opportunity to review past and current work of Deborah Dultzin & collaborators on the emitting regions in quasars, to which this paper – given the vastness of the subject – is limited.

REFERENCES

Bachev, R., Marziani, P., Sulentic, J. W., Zamanov, R., Calvani, M., & Dultzin-Hacyan, D. 2004, ApJ, 617, 171
Collin, S., Kawaguchi, T., Peterson, B. M., & Vestergaard, M. 2006, A&A, 456, 75
Cox, D. P. 2000, RevMexAA (SC), 9, 337
Dultzin-Hacyan, D., Marziani, P., & Sulentic, J. W. 2000, RevMexAA (SC), 9, 308
Ferland, G. J., et al. 1998, PASP, 110, 761
Horne, K., Peterson, B. M., Collier, S. J., & Netzer, H. 2004, PASP, 116, 465
Kollatschny, W. 2003, A&A, 407, 461
Korista, K. T., et al. 1995, ApJS, 97, 285
Marziani, P., Sulentic, J. W., Zwitter, T., Dultzin-Hacyan, D., & Calvani, M. 2001, ApJ, 558, 553
Marziani, P., Sulentic, J. W., Dultzin-Hacyan, D., Calvani, M., & Moles, M. 1996, ApJS, 104, 37
Marziani, P., Sulentic, J. W., Zamanov, R., Calvani, M., Dultzin-Hacyan, D., Bachev, R., & Zwitter, T. 2003a, ApJS, 145, 199
Marziani, P., Zamanov, R., Sulentic, J. W., & Calvani, M. 2003b, MNRAS, 345, 1133
Popović, L. Č., Mediavilla, E., Bon, E., & Ilić, D. 2004, A&A, 423, 909
Strateva, I. V., et al. 2003, AJ, 126, 1720
Sulentic, J. W., Bachev, R., Marziani, P., Negrete, C. A., & Dultzin, D. 2007, ApJ, 666, 757
Sulentic, J. W., Marziani, P., & Dultzin-Hacyan, D. 2000, ARA&A, 38, 521
Sulentic, J. W., Marziani, P., Zamanov, R., Bachev, R., Calvani, M., & Dultzin-Hacyan, D. 2002, ApJ, 566, L71
Sulentic, J. W., Repetto, P., Stirpe, G. M., Marziani, P., Dultzin-Hacyan, D., & Calvani, M. 2006, A&A, 456, 929
Sulentic, J. W., Stirpe, G. M., Marziani, P., Zamanov, R., Calvani, M., & Braito, V. 2004, A&A, 423, 121
Sulentic, J. W., Zamfir, S., Marziani, P., Bachev, R., Calvani, M., & Dultzin-Hacyan, D. 2003, ApJ, 597, L17
Sulentic, J. W., Zheng, W., Calvani, M., & Marziani, P. 1990, ApJ, 355, L15
Verner, E. M., Verner, D. A., Korista, K. T., Ferguson, J. W., Hamann, F., & Ferland, G. J. 1999, ApJS, 120, 101
Véron-Cetty, M.-P., Joly, M., & Véron, P. 2004, A&A, 417, 515
Wu, X.-B., & Liu, F. K. 2004, ApJ, 614, 91